DOI: 10.1002/ejic.200601002

New Ternary Complexes of Copper(II) with 2,2′-Bipyridine (Bpy) and Phosphocholine (PCh^-) or the Quaternary 1-(2-Phosphonomethoxy)ethyl Derivative of 2,4-Diaminopyrimidine ($PMEDAPy^-$)

Alfonso Fernández-Botello,[a] Albert Escuer,[a] Xavier Solans,[b] Mercè Font-Bardía,[b] Antonin Holý,[c] Helmut Sigel,[d] and Virtudes Moreno*[a]

Keywords: Ternary complexes / Oxido bridges / Phosphonate bridges / Copper(II) / Magnetic properties

The polynuclear Cu^{II} complexes $[Cu_4Cl_2(bpy)_4(PCh^-)_2](ClO_4)_4\cdot H_2O$ (**1**) and $[Cu_6(bpy)_6(PMEAPy^-)_4](ClO_4)_8\cdot 2H_2O$ (**2**), where bpy = 2,2′-bipyridine, PCh^- = phosphocholine {[2-(phosphonooxy)ethyl]trimethylammonium} and $PMEDAPy^-$ = 1-[2-(phosphonomethoxy)ethyl]-2,4-diaminopyrimidine, have been synthesized and characterized by X-ray single-crystal analysis. Compound **1** crystallizes in the triclinic system (*P*-1 space group) and consists of tetranuclear Cu^{II} units, which are threefoldly bridged by μ_3-*O,O′,O′′*-phosphate groups in a square arrangement around the copper atoms. Complex **2** crystallizes in the monoclinic system ($P2_1/c$ space group) and consists of hexanuclear Cu^{II} units containing the same kind of μ_3-phosph(on)ate bridges like **1** and in addition μ_4-*O,O′,O′′,O′′*-phosphonate bridges. The topology of compound **2** can be envisaged as two triangular subunits linked by means of a double Cu–O–Cu bridge provided by the μ_4-phosphonate unit. Magnetic susceptibility measurements of the two complexes in the temperature range of 2–300 K show weak antiferromagnetic couplings mediated by the phosph(on)ate bridges.

Introduction

Solid metal phosphates and phosphonates are receiving much attention[1,2] because of their interesting magnetic and electronic properties.[3] They also have promising potential for applications in different areas: supports for catalysts,[4] as sensors[5], and in nonlinear optics.[6] This diversity in applications is a reflection of their diversity in structure and composition which is characteristic for these compounds.

Moreover, the two phosph(on)ate ligands considered in this study are also of biological relevance: phosphocholine (PCh^-), also known as 2-(trimethylammonio)ethyl phosphate and [2-(phosphonooxy)ethyl]trimethylammonium (Figure 1), is a fundamental cell metabolite.[7] The quaternary 1-[2-(phosphonomethoxy)ethyl] derivative of 2,4-diaminopyrimidine (Figure 1) is also named 1-[2-(phosphonomethoxy)ethyl]-2,4-diaminopyrimidine ($PMEDAPy^-$)[8] to indicate its structural relationship to several other acyclic nucleotide analogues which show antiviral properties.[9–11] Metal ion complexes of both phosph(on)ate ligands (Figure 1), or at least close relatives, have already been studied in aqueous solution and their corresponding isomeric equilibria were quantified.[8,11,12] Indeed, for the ternary complexes of $PMEDAPy^-$ with Cu^{2+} and 2,2′-bipyridine (bpy) or 1,10-phenanthroline (phen) intramolecular stacking interactions in solution could be established.[8] Knowledge of such weak interactions is important in order to understand biological interactions better, e.g. in structures of proteins, active-site cavities and in many low-molecular-weight

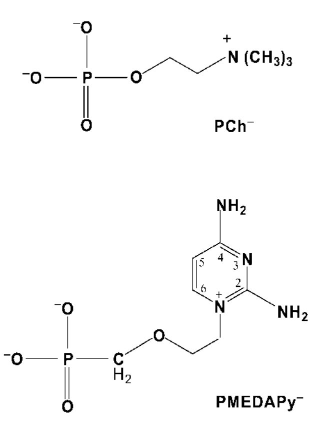

Figure 1. Chemical structures of the anions of phosphocholine (PCh^-) and 2,4-diamino-1-[2-(phosphonomethoxy)ethyl]pyrimidine ($PMEDAPy^-$; see also the second paragraph of the Introduction).

---

[a] Departament de Química Inorgànica, Universitat de Barcelona,
Martí i Franqués 1–11, 08028 Barcelona, Spain
Fax: +34-93-4907725
E-mail: albert.escuer@qi.ub.es
virtudes.moreno@qi.ub.es
[b] Departament de Cristallografía, Mineralogia i Dipòsits Minerals, Universitat de Barcelona,
Martí Franqués s/n, 08028, Barcelona, Spain
[c] Academy of Sciences, Institute of Organic Chemistry and Biochemistry,
16610 Prague, Czech Republic
[d] Department of Chemistry, Inorganic Chemistry, University of Basel,
Spitalstrasse 51, 4056 Basel, Switzerland

mixed-ligand complexes,[13] also their relevance for the stability of DNA, which depends much on the stacking interactions of the nucleobases.[14]

Of course, the biological role of copper is nowadays well established: copper-containing enzymes and proteins are widely distributed in plants and animals,[15] the metal ion being present in the form of ternary or polynuclear complexes.[15,16] For example, exchange-coupled polynuclear Cu^{II} complexes are of relevance in biological processes involving laccase, a metalloprotein which belongs to the family of multicopper oxidases. Laccase contains four copper ions which are coupled to four one-electron substrate oxidations, i.e. the reduction of dioxygen to water.[17,18]

For the various reasons indicated above, we studied ternary Cu^{II} complexes of the phosph(on)ate ligands (Figure 1) in the solid state by employing 2,2′-bipyridine as the second ligand. The syntheses, X-ray crystal structure analyses and magnetic properties of two polynuclear Cu^{II} complexes, $[Cu_4Cl_2(bpy)_4(PCh^-)_2](ClO_4)_4\cdot H_2O$ (**1**) and $[Cu_6(bpy)_6(PMEDAPy^-)_4](ClO_4)_8\cdot 2H_2O$ (**2**), are now presented. In **1** PCh^- acts as tridentate μ_3-*O,O′,O′′*-bridging ligand, whereas in **2** one half of the $PMEDAPy^-$ ligands acts in a similar way, but the other half forms a tetradentate μ_4-*O,O′,O′′,O′′*-phosphonate bridge. It needs to be emphasized that these coordination modes are quite unusual for phosph(on)ate bridges.

Complexes with large M–O–X–O–M bridges formed by tetrahedral anions like sulfate or phosphate show typically weak magnetic interactions[19] and indeed, compounds **1** and **2**, containing exclusively M–O–P–O–M phosph(on)ato bridges, show a moderately weak antiferromagnetic coupling. In the last few years there is a growing interest in this kind of structural units because of their ability to generate high nuclearity cages with a variety of first row transition cations. Phosph(on)ato ligands can bind up to six metallic centers and, combined with other bridges (mainly hydroxo or alkoxo derivatives), they are able to give high nuclearity systems containing, e.g. Co_{13}, Mn_{12}, Fe_9, Co_8 or Mn_6.[20] Interesting magnetic properties such as the single molecule magnet (SMM) response have been characterized for some of them.

Results and Discussion

The reaction of $[Cu(ClO_4)_2]\cdot 6H_2O$ with 2,2′-bipyridine (bpy) and phosphocholine (PCh^-) or 1-[2-(phosphonomethoxy)ethyl]-2,4-diaminopyrimidine ($PMEDAPy^-$) in water with addition of HCl afforded crystals of the complexes $[Cu_4Cl_2(bpy)_4(PCh^-)_2](ClO_4)_4\cdot H_2O$ (**1**) and $[Cu_6(bpy)_6(PMEDAPy^-)_4](ClO_4)_8\cdot 2H_2O$ (**2**) after two or four weeks of evaporation at room temperature, respectively. The crystals were suitable to be studied by X-ray diffraction.

Crystal Structures

$[Cu_4Cl_2(bpy)_4(PCh^-)_2](ClO_4)_4\cdot H_2O$ (1)

A labeled ORTEP plot of the structure is shown in Figure 2. Selected bond lengths and angles are reported in Table 1 and Table 2, respectively. The structure of the compound consists of a tetranuclear centrosymmetric ternary Cu^{II} complex with bpy and PCh^- as ligands. There are two nonequivalent complexes with the same structure and similar bond parameters in the asymmetric unit of **1**; the following description corresponds to one of them. The Cu1 atoms are pentacoordinated, with a polyhedral arrangement close to a square-pyramidal geometry, where the equatorial plane is defined by two nitrogen (bpy) atoms and two oxygen (phosphate) atoms; one chloride is in the apical position. For Cu2 the main plane is defined by two nitrogen (bpy), one chloride and one oxygen (phosphate) with a water molecule in the axial position. In both cases, the metal ion is above the equatorial plane (see Table 2 for bond angles). The equatorial bond lengths to the *O*-phosphate atoms lie within the short range between 1.899(5) and 1.960(4) Å.

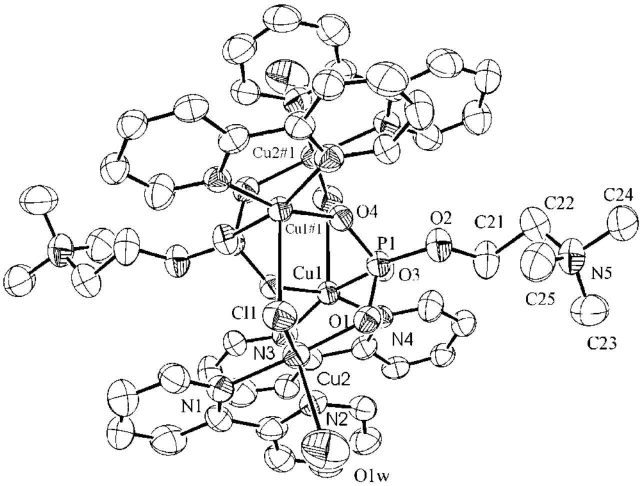

Figure 2. Labeled ORTEP plot (ellipsoid probability 30%) for one of the two nonequivalent units of $[Cu_4Cl_2(bpy)_4(PCh^-)_2](ClO_4)_4\cdot H_2O$ (**1**).

Table 1. Selected bond lengths [Å] $[Cu_4Cl_2(bpy)_4(PCh^-)_2](ClO_4)_4\cdot H_2O$ (**1**).[a]

Cu1–N3	2.026(6)	Cu3–N7	2.021(6)
Cu1–N4	1.947(6)	Cu3–N6	1.974(6)
Cu1–O3	1.925(5)	Cu3–O7	1.911(5)
Cu1–O4#1**	1.920(5)	Cu3–O8#2*	1.960(4)
Cu1–Cl1#1**	2.677(2)	Cu3–Cl2	2.666(2)
Cu2–N1	2.002(6)	Cu4–N8	1.977(6)
Cu2–N2	2.020(7)	Cu4–N9	1.982(6)
Cu2–O1	1.899(5)	Cu4–O5	1.926(5)
Cu2–Cl1	2.269(3)	Cu4–Cl2	2.319(2)
Cu2–O1w	2.64(1)	Cu4–O8#2*	2.350(5)

[a] Symmetry transformations used to generate equivalent atoms: * $-x + 1, -y, -z + 1$; ** $-x + 2, -y + 1, -z$.

The four Cu^{II} ions of the tetranuclear unit define a ring (Figure 3) which is held together by threefold bridged μ_3-*O,O′,O′′*-phosphate groups. The Cu1···Cu1#1 distance is 4.9967(15) Å, whereas the side-ring distances are 3.8573(15) and 3.5830(13) Å, and thus smaller than the Cu···Cu distances in related dinuclear complexes.[21,22]

Table 2. Selected angles [°] for$[Cu_4Cl_2(bpy)_4(PCh^-)_2](ClO_4)_4{\cdot}H_2O$ (**1**).[a]

O3A–Cu2A–O4A*	94.0(2)	C15A–N3A–Cu1A	112.6(5)
O3A–Cu2A–N1A	90.0(2)	C16A–N4A–Cu1A	112.7(5)
O4A*–Cu2A–N1A	172.8(3)	C20A–N4A–Cu1A	126.9(5)
O3A–Cu2A–N2A	166.2(3)	O4**–Cu1–O3	94.0(2)
O4A*–Cu2A–N2A	94.1(2)	O4**–Cu1–N4	165.8(2)
N1A–Cu2A–N2A	80.9(3)	O3–Cu1–N4	90.8(2)
O3A–Cu2A–Cl1A	92.5(1)	O4**–Cu1–N3	91.9(2)
O4A*–Cu2A–Cl1A	82.2(2)	O3–Cu1–N3	166.1(2)
N1A–Cu2A–Cl1A	103.6(2)	N4–Cu1–N3	80.6(3)
N2A–Cu2A–Cl1A	99.6(2)	O4**–Cu1–Cl1**	100.4(2)
O1A–Cu1A–N3A	170.2(2)	O3–Cu1–Cl1**	86.4(1)
O1A–Cu1A–N4A	91.2(2)	N4–Cu1–Cl1**	93.3(2)
N3A–Cu1A–N4A	81.3(3)	N3–Cu1–Cl1**	104.9(2)
O1A–Cu1A–Cl1A	94.0(1)	O1–Cu2–N1	170.9(3)
N3A–Cu1A–Cl1A	95.5(2)	O1–Cu2–N2	92.7(3)
N4A–Cu1A–Cl1A	153.0(2)	N1–Cu2–N2	82.2(3)
O1A–Cu1A–O4A*	88.8(2)	O1–Cu2–Cl1	90.6(2)
N3A–Cu1A–O4A*	90.2(2)	N1–Cu2–Cl1	96.1(2)
N4A–Cu1A–O4A*	123.9(2)	N2–Cu2–Cl1	166.6(2)
Cl1A–Cu1A–O4A*	82.7(1)	Cu2–Cl1–Cu1**	92.5(9)
Cu1A–Cl1A–Cu2A	84.1(7)	P1–O1–Cu2	126.8(3)
P1A–O1A–Cu1A	129.7(3)	P1–O3–Cu1	125.9(3)
P1A–O3A–Cu2A	126.5(3)	P1–O5–Cu1**	135.9(3)
P1A–O4A–Cu2A*	125.7(3)	C1–N1–Cu2	130.2(6)
P1A–O4A–Cu1A*	121.3(2)	C5–N1–Cu2	111.5(5)
Cu2A*–O4A–Cu1A*	101.5(2)	C6–N2–Cu2	116.4(6)
C1A–N1A–Cu2A	123.0(5)	C10–N2–Cu2	124.2(5)
C5A–N1A–Cu2A	114.0(5)	C15–N3–Cu1	115.3(5)
C6A–N2A–Cu2A	113.5(5)	C11–N3–Cu1	125.7(6)
C10A–N2A–Cu2A	123.9(5)	C20–N4–Cu1	127.4(6)
C11A–N3A–Cu1A	126.2(5)	C16–N4–Cu1	115.7(5)

[a] Symmetry transformations used to generate equivalent atoms: * $-x + 1, -y, -z + 1$ ** $-x + 2, -y + 1, -z$.

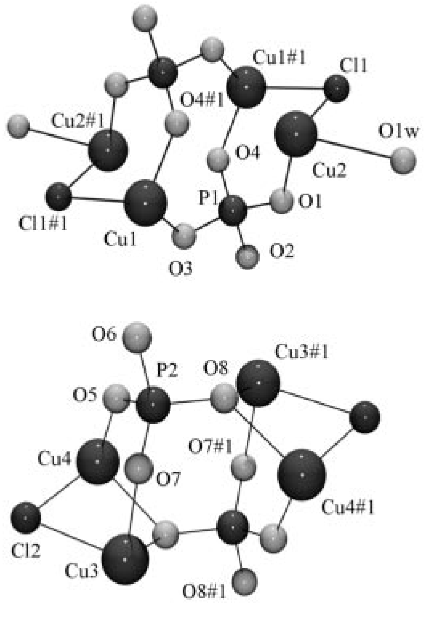

Figure 3. Plot of the Cu_4 arrangement for the core of the two nonequivalent units of **1**.

The distances between the two planes defined by the bipyridine ligands are in the range of 4.499(5) to 5.085(4) Å; this is longer than the distances for stacking interactions, which are usually between 3.3 and 3.8 Å.[23] Thus, the existence of a stacking interaction must be ruled out in this case. In Figure 3 a schematic representation of the four-copper atom core is shown for the two nonequivalent units.

$[Cu_6(bpy)_6(PMEDAPy^-)_4](ClO_4)_8{\cdot}2H_2O$ (2)

A labeled ORTEP plot of the structure is shown in Figure 4. Selected bond lengths and angles are reported in Table 3 and Table 4, respectively. The structure of the compound consists of a hexanuclear Cu^{II} ternary complex with bpy and $PMEDAPy^-$ as ligands. Two of the copper atoms are pentacoordinated, with a polyhedral arrangement close to a square-pyramidal geometry, where the equatorial positions are occupied by two nitrogen (bpy) and two oxygen (phosphonate) atoms, and the apical position by one oxygen (phosphonate) atom or one water molecule. The bond lengths for the equatorial position are in the range of 1.887(2)–1.993(2) Å (typical bond lengths), and the bond lengths for the apical position are 2.220(2) Å for Cu3–O8 and 2.486(4) Å for Cu2–O1w. In both cases, the copper

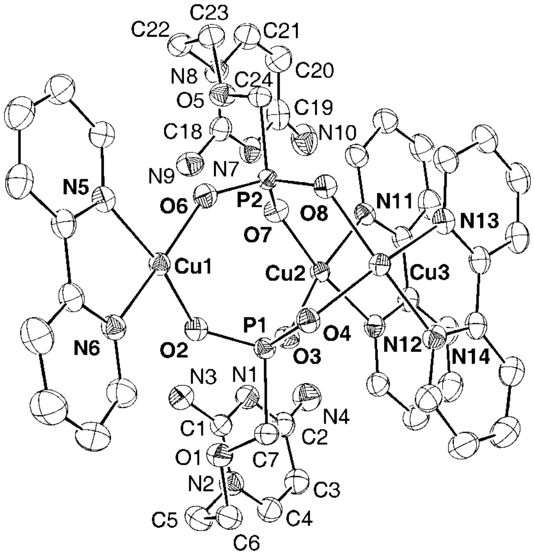

Figure 4. Labeled ORTEP plot (ellipsoid probability 30%) for the asymmetric unit of $[Cu_6(bpy)_6(PMEDAPy^-)_4](ClO_4)_8{\cdot}2H_2O$ (**2**). Oxygen atoms above Cu3 and Cu2 are omitted for clarity.

Table 3. Selected bond lengths [Å] for $[Cu_6(bpy)_6(PMEDAPy^-)_4](ClO_4)_8{\cdot}2H_2O$ (**2**).[a]

Cu1–O6	1.887(2)	P1–O2	1.519(2)
Cu1–O2	1.919(2)	P1–O3	1.524(2)
Cu1–N6	1.986(3)	P1–O4	1.516(2)
Cu1–N5	1.990(3)	O1–C6	1.445(5)
Cu2–O3	1.917(2)	O1–C7	1.416(4)
Cu2–O7	1.918(2)	P2–O6	1.512(2)
Cu2–N12	1.997(6)	P2–O8	1.528(2)
Cu2–N11	2.003(2)	P2–O7	1.497(2)
Cu3–O4	1.941(2)	O5–C23	1.402(4)
Cu3–N14	1.977(3)	O5–C24	1.420(4)
Cu3–O8	1.993(2)		
Cu3–N13	2.002(3)		
Cu3–O8*	2.220(2)		

[a] Symmetry transformations used to generate equivalent atoms: * $-x, -y, -z$.

atoms are always above the equatorial plane. Cu1 atom is placed in a distorted square planar environment.

Table 4. Selected angles [°] for $[Cu_6(bpy)_6(PMEDAPy^-)_4](ClO_4)_8 \cdot 2H_2O$ (**2**).[a]

O6–Cu1–O2	96.09(10)	O8–Cu3–O8*	84.54(08)
O6–Cu1–N6	165.97(12)	N13–Cu3–O8*	101.50(09)
O2–Cu1–N6	94.53(11)	P1–O2–Cu1	128.14(15)
O6–Cu1–N5	89.84(11)	P1–O3–Cu2	135.76(15)
O2–Cu1–N5	169.39(10)	P1–O4–Cu3	124.86(13)
N6–Cu1–N5	81.16(11)	P2–O6–Cu1	142.93(16)
O3–Cu2–O7	93.79(10)	P2–O7–Cu2	143.31(15)
O3–Cu2–N12	91.14(11)	P2–O8–Cu3*	136.44(13)
O7–Cu2–N12	171.26(10)	Cu3–O8–Cu3*	95.46(08)
O3–Cu2–N11	170.44(11)	C8–N5–Cu1	125.00(02)
O7–Cu2–N11	93.81(11)	C12–N5–Cu1	115.70(02)
N12–Cu2–N11	80.61(11)	C17–N6–Cu1	127.10(03)
O4–Cu3–N14	92.14(11)	C13–N6–Cu1	113.60(02)
O4–Cu3–O8	92.02(09)	C29–N11–Cu2	114.40(02)
N14–Cu3–O8	170.80(10)	C25–N11–Cu2	125.00(02)
O4–Cu3–N13	159.69(10)	C34–N12–Cu2	126.20(02)
N14–Cu3–N13	80.38(12)	C30–N12–Cu2	114.20(02)
O8–Cu3–N13	92.97(10)	C39–N13–Cu3	113.90(02)
O4–Cu3–O8*	98.57(08)	C35–N13–Cu3	125.30(02)
N14–Cu3–O8*	102.94(10)	C40–N14–Cu3	115.70(02)
		C44–N14–Cu3	125.40(03)

[a] Symmetry transformations used to generate equivalent atoms: * –*x*, –*y*, –*z*.

The compound can be envisaged as two trinuclear subunits linked by means of a double oxido bridge. The Cu3···Cu3* distance is 3.1218(6) Å, whereas the distance between the metal ions Cu2 and Cu3 (see Figure 5) is 3.3268(6) Å; it means that this distance is shorter than the Cu···Cu distances in dinuclear complexes.[21,22] A schematic representation of the core environment for the six copper atoms of **2**, including the bridging phosphonate groups, is shown in Figure 5.

This compound exhibits both intra and intermolecular π–π interactions. Intramolecular stacking can be observed for the heteroaromatic rings including N11 and N13, where the distance between the centroids is 3.57 Å (see Figure 4); this distance is in the expected order.[13,24] Intermolecular interactions are found between the pyridine ring including N6 and the diaminopyrimidine ring including N7/N8 of the neighboring hexanuclear unit with the distance between the centroids of 3.51 Å. These interactions give a supramolecular 1D arrangement of the Cu_6 molecules along the [010] direction (Figure 6). Hence, these observations in the solid state confirm the results obtained in aqueous solution for the ternary $Cu(bpy)(PMEDAPy)^+$ and $Cu(phen)(PMEDAPy)^+$ complexes; the formation degree of the intramolecular stacks amounts in these species in solution to about 69 and 77 %, respectively.[8] It is not surprising that in the solid state stacking between bpy and the pyrimidine ring occurs in an inter- and not in an intramolecular fashion; crystal packing affects such weak interactions.[24] Indeed, similar differences between the stacking properties in solution and in the solid state have been observed before.[13,24]

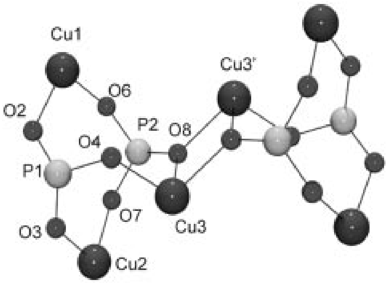

Figure 5. Plot of the core environment for the Cu_6 unit of compound **2**.

Magnetic Behavior

Experimental susceptibility data indicate that the $\chi_M \cdot T$ product for both compounds exhibits a quasi constant value between room temperature and 100 K. Below this temperature it decreases, approaching zero at very low temperatures, which indicates a weak antiferromagnetic coupling. For compound **1** the $\chi_M \cdot T$ value at room temperature is $1.73\ cm^3 \cdot K \cdot mol^{-1}$ and in good agreement with four isolated Cu^{II} ions (the expected value for g = 2.00 is

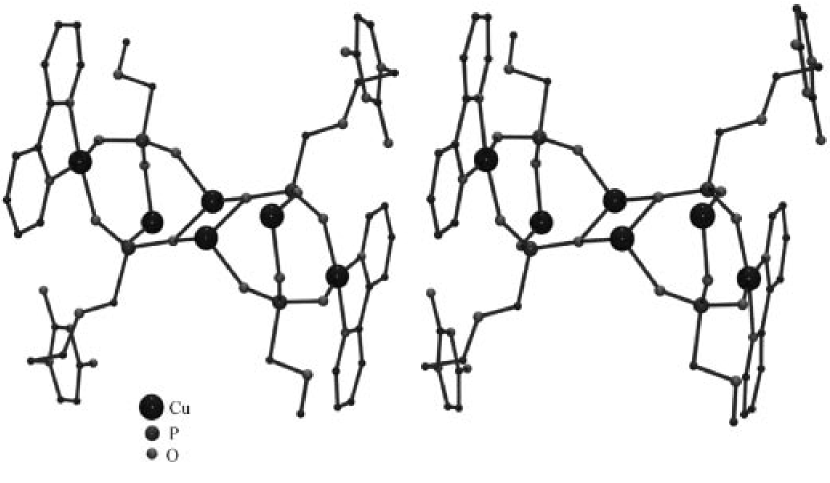

Figure 6. Plot of two Cu_6 units showing the π–π stacking between one of the bpy and one of the diaminopyrimidine rings. For clarity, the noninteracting aromatic rings are not plotted.

1.5 $cm^3 \cdot K \cdot mol^{-1}$). The χ_M vs. T plot shows a maximum of susceptibility around 4 K (see Figure 7). The $\chi_M \cdot T$ value of 2.67 $cm^3 \cdot K \cdot mol^{-1}$ at room temperature for compound **2** is slightly greater than the spin only value of 2.25 $cm^3 \cdot K \cdot mol^{-1}$ expected for six Cu^{II} ions (see Figure 8).

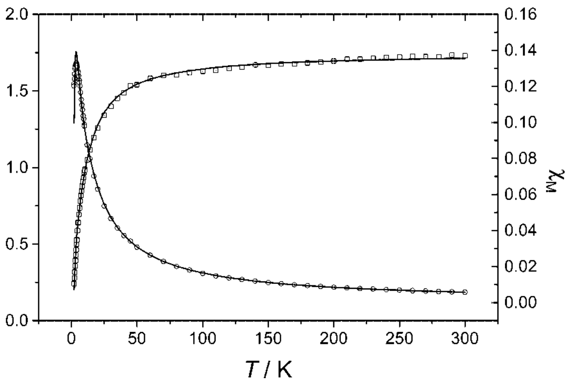

Figure 7. Plot of $\chi_M \cdot T$ vs. T (open squares) and χ_M vs. T (open circles) for compound $[Cu_4Cl_2(bpy)_4(PCh^-)_2](ClO_4)_4 \cdot H_2O$ (**1**). Solid lines show the best fit of the experimental data.

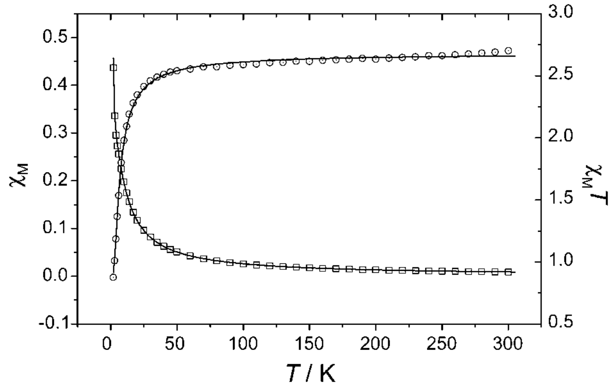

Figure 8. Plot of $\chi_M \cdot T$ vs. T (open circles) and χ_M vs. T (open squares) for compound $[Cu_6(bpy)_6(PMEDAPy^-)_4]$ $(ClO_4)_8 \cdot 2H_2O$ (**2**). Solid lines show the best fit obtained (see text).

A fit of the experimental susceptibility data for **1** was performed on the basis of the three coupling constants seen in the interaction Scheme 1.

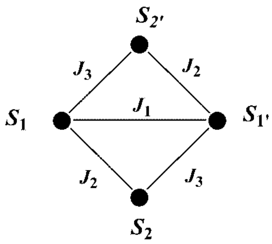

Scheme 1.

J_1 corresponds to the double OPO bridge with medium torsion angles, J_2 to the single bridge with low torsion angles, and J_3 to the single bridge with large torsion. The same Scheme is common for the two nonequivalent molecules present in the structure, which show only a minor difference in the torsion related to J_2. The best fit obtained by means of the CLUMAG program, based in the irreducible tensor operator formalism (ITO) on the Hamiltonian $H = -J_1(S_1 \cdot S_{1'}) - J_2(S_1S_2 + S_{1'} \cdot S_{2'}) - J_3(S_{1'} \cdot S_{2'} + S_{1'} \cdot S_2)$, gives the values $J_1 = -9.7$ cm^{-1}, $J_2 = -4.2$ cm^{-1}, $J_3 = -7.5$ cm^{-1}, and $g = 2.157$. A second fit performed assuming $J_2 = J_3$ gives a similar J_1 value ($J_1 = -8.7$ cm^{-1}) and an average value for $J_2 = J_3$ of 6.3 cm^{-1}.

The interaction Scheme for compound **2** consists of seven different interactions (Scheme 2). A negligible or very weak interaction can be expected for the superexchange pathway J_4 which relates the Cu^{II} centers by means of an axial–equatorial double oxido bridge. Also, intermolecular interactions mediated by the π–π stacking should be negligible, because the rings involved in this interaction are placed far from the copper atoms.

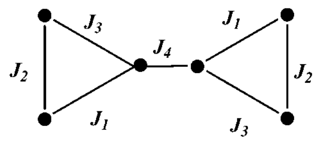

Scheme 2.

The three remaining interactions correspond to doubly $Cu-(OPO)_2-Cu$ bridged fragments, which display large differences within the bond parameters, specially for the Cu–O–O–Cu torsion angles. Trying to fit a weakly coupled system (without susceptibility maximum) with four coupling constants does not make mathematical sense, because many local minima can be found in the least-squares process. Therefore, to avoid overparametrization the experimental data for this compound were fitted assuming an average J value and neglecting the axial–equatorial interaction between the triangular units. The best fit under these conditions, performed by applying the Hamiltonian $H = -J(S_1S_2 + S_2S_3 + S_1S_3)$, gives the values $J = -4.1$ cm^{-1} and $g = 2.180$. Fits including the interaction between the two triangular units gave negligible values for this constant, which is closer to the $\chi_M \cdot T$ value at low T of two independent Cu^{II} ions rather than an S = 0 ground state.

These results are in good agreement with related compounds containing the phosphonato ligand in its η_3-O,O',O'' coordination mode, for which superexchange interactions are typically in the range of –5 to –10 cm^{-1}.[25]

Experimental Section

Caution! *Perchlorate salts of metal complexes with organic ligands are potentially explosive. Only a small amount of the material should be prepared and it should be handled with extreme care.*

$[Cu_4Cl_2(bpy)_4(PCh^-)_2](ClO_4)_4 \cdot H_2O$ (1): $[Cu(ClO_4)_2] \cdot 6H_2O$ (1 mmol), 2,2′-bipyridine (1 mmol) and [2-(phosphonooxy)ethyl]-trimethylammonium chloride (= phosphocholine; PCh^-) (0.5 mmol), obtained from Fluka (Buchs, Switzerland), were mixed in distilled water (20 mL) and stirred for 48 h at room temperature. A few drops of 1 M HCl were then added to the solution. Single dark-blue crystals of **1** suitable for X-ray crystallography were formed by evaporation at room temperature after two weeks.

Table 5. Crystal data and summary of data collection and refinement for $[Cu_4Cl_2(bpy)_4(PCh^-)_2](ClO_4)_4 \cdot H_2O$ (**1**) and $[Cu_6(bpy)_6(PMEDAPy^-)_4](ClO_4)_8 \cdot 2H_2O$ (**2**).

	1	**2**
Empirical formula	$C_{50}H_{60}C_{16}Cu_4N_{10}O_{25}P_2$	$C_{88}H_{100}Cl_8Cu_6N_{28}O_{52}P_4$
Wavelength [Å]	0.71069	0.71073
T [K]	293(2)	293(2)
θ range [°]	1.64 to 31.65	1.73 to 31.57
hkl ranges	–16 to 16, –15 to 13, 0 to 33	–25 to 23, 0 to 17, 0 to 41
Crystal system, space group	triclinic, $P\bar{1}$	monoclinic, $P2_1/c$
Crystal dimensions [mm]	$0.1 \times 0.1 \times 0.2$	$0.1 \times 0.1 \times 0.2$
a [Å]	12.4230(10)	17.5970(10)
b [Å]	12.7080(10)	13.2460(10)
c [Å]	22.7730(10)	28.5280(10)
α [°]	98.534(8)	90
β [°]	99.296(8)	115.076(8)
δ [°]	98.303(8)	90
Volume [Å^3]	3456.1(4)	6022.8(9)
Absorption coefficient [mm^{-1}]	1.576	1.377
Reflections collected/unique	15246/9819 [R(int) = 0.0370]	52896/17121 [R(int) = 0.0259]
Data/restraints/parameters	9819/222/846	17121/0/839
Goodness-of-fit on F_2	0.988	1.073
Final R indices [$I > 2\sigma(I)$]	$R_1 = 0.0701$, $wR_2 = 0.2103$	$R_1 = 0.0538$, $wR_2 = 0.1680$
R indices (all data)	$R_1 = 0.1271$, $wR_2 = 0.2353$	$R_1 = 0.0746$, $wR_2 = 0.2244$
Extinction coefficient	0.0034(10)	0.0022(6)
Largest diff. peak and hole/e·Å^{-3}	0.633 and –0.554	0.794 and –0.744

(Yield: 64%). Calculated for $C_{50}H_{60}Cl_6Cu_4N_{10}O_{25}P_2$: C 34.68, N 8.09, H 3.47; found C 35.60, N 8.29, H 3.27%.

$[Cu_6(bpy)_6(PMEDAPy^-)_4](ClO_4)_8 \cdot 2H_2O$ (2): $[Cu(ClO_4)_2] \cdot 6H_2O$ (1 mmol), 2,2′-bipyridine (1 mmol) and 2,4-diamino-1-[2-(phosphonomethoxy)ethyl]pyrimidine·HCl (0.5 mmol), which was synthesized as described in the literature,[26] were mixed in distilled water and acetonitrile (15 mL:10 mL) and stirred for 24 h at room temperature. A few drops of 1 M HCl were then added to the solution. Single blue crystals of **2** suitable for X-ray crystallography were formed by evaporation at room temperature after four weeks. (Yield: 73%). Calculated for $C_{88}H_{100}Cl_8Cu_6N_{28}O_{52}P_4$: C 33.31, N 12.36, H 3.15; found C, 33.82, N 12.47, H 3.06%.

Magnetic Measurements: Magnetic susceptibility measurements were carried out for **1** and **2** on microcrystalline samples with a Quantum Design SQUID MPMS5 magnetometer working in the range of 2–300 K under magnetic fields of 7000 G. Application of Pascal's constant was used for diamagnetic corrections. The magnetic measurements were carried out by the Magnetochemistry Services of the University of Barcelona.

Crystal-Structure Determination: The X-ray single-crystal data for **1** and **2** were collected on a MAR345 diffractometer with an image plate detector. Crystal size: $0.1 \times 0.1 \times 0.2$ mm. The crystallographic data, conditions used for the intensity data collection, and some features of the structure refinement are listed in Table 5. Unit-cell parameters were determined from 8505 reflections ($3 < \theta < 30°$) in the case of complex **1** and 42513 reflections ($3 < \theta < 31°$) for complex **2**. Both cases were refined by the least-squares method. Intensities were collected with graphite-monochromatized Mo-K_α radiation. 15246 reflections were measured in the range $1.64 \leq \theta \leq 31.65$ and 52896 reflections were measured in the range $1.73 \leq \theta \leq 31.57$ for complex **1** and **2**, respectively. 9819 (complex **1**) and 17121 (complex **2**) reflections were nonequivalent by symmetry [R(int) (on I) = 0.037 and 0.025 for complex **1** and **2**, respectively]. For complex **1** 5385 reflections were assumed as observed applying the condition $I > 2\sigma(I)$. In the case of complex **2**, 13652 reflections were assumed as observed applying to the condition $I > 2\sigma(I)$. The Lorentz polarization was corrected but no absorption corrections were made in both cases.

The structures were solved by direct methods with the SHELXS computer program[27] and refined by the full-matrix least-squares method (SHELX97 program[27]) using 9819 reflections for complex **1** and 17121 reflections for complex **2** (very negative intensities were not assumed). The minimized function was $\Sigma w||F^o|^2 - |F_c|^2|^2$, where $w = [\sigma^2(I) + (0.1582P)^2]^{-1}$, and $P = (|F_o|^2 + 2|F_c|^2)/3$ in the case of complex **1**. For complex **2** $w = [\sigma^2(I) + (0.1630P)^2 + 1.6389P]^{-1}$, and $P = (|F_o|^2 + 2|F_c|^2)/3$. In both cases, f, f', and f'' were taken from ref.[28].

All H atoms were computed and refined by a riding model, with an isotropic thermal parameter equal to 1.2 times the equivalent thermal parameter of the C linked to H. The final R (on F) factor was 0.070 and 0.054, wR (on $|F|^2$) = 0.210 and 0.168 and goodness of fit was 1.017 and 1.073 for complexes **1** and **2**, respectively, for all observed reflections. For complex **1**, the number of refined parameters was 846. As the ratio number of observed reflections/number of refined parameters was low, oxygen atoms of perchlorate ions were only refined isotropically with bond lengths and angles constrained to have the same value. Max. shift/esd. = 0.00, mean shift/esd. = 0.00. Max. and min. peaks in the final difference synthesis was 0.633 and –0.554 e·Å^{-3}, respectively. For complex **2**, the number of refined parameters was 839. Max. shift/esd. = 0.00, mean shift/esd = 0.00. Max. and min. peaks in the final difference synthesis was 0.794 and –0.744 e·Å^{-3}, respectively.

CCDC-624676 and -624677 contain the supplementary crystallographic data for this paper. These data can be obtained free of charge from the Cambridge Crystallographic Data Centre via www.ccdc.cam.ac.uk/data@request/cif.

Acknowledgments

The authors thank COST D20 (Brussels and Bern), the Ministerio de Ciencia y Tecnología (MCYT) (ref. BQU-2002-00601) as well as the University of Barcelona (grant to A. F. B.) and the University of Basel (grant to H. S.) for financial support.

---

[1] Y. Song, N. A. Chernova, P. Y. Zavalij, M. S. Whittingham, *Materials Research Society Symposium Proceedings* **2002**, *755*, 75–80.
[2] W. J. Chang, C. Y. Chen, K. H. Lii, *Solid State Chem.* **2003**, *172*, 6–11.
[3] J. E. Greedan, K. Reubenbauer, T. Birchall, M. Ehlert, D. R. Corbin, M. A. Subramanian, *Solid State Chem.* **1988**, *77*, 376–388.
[4] R. A. W. Johnstone, J. Y. Liu, L. Lu, D. Whittaker, *J. Mol. Catal. A J. Mol. Catal.* **2003**, *191*, 289–294.
[5] M. Shiotsuka, S. Takase, Y. Shimizu, *Chem. Sens.* **2001**, *17*, 381–383.
[6] S. B. Ungashe, W. L. Wilson, H. E. Katz, G. R. Scheller, T. M. Putvinski, *J. Am. Chem. Soc.* **1992**, *114*, 8717–8719.
[7] a) J. D. Rawn, *Biochemistry*, Patterson, Burlington, NC (USA), **1989**, pp. 213–216 and 541–544; b) L. Stryer, *Biochemie* (translated by B. Pfeiffer and J. Guglielmi from *Biochemistry*, W. H. Freeman & Co., New York, **1988**), Spektrum Akad. Verlag, Heidelberg, **1991**, pp. 296–299 and 574–577.
[8] A. Fernández-Botello, A. Holý, V. Moreno, H. Sigel, *Polyhedron* **2003**, *22*, 1067–1076.
[9] a) A. Holý, I. Votruba, M. Masojídková, G. Andrei, R. Snoeck, L. Naesens, E. De Clercq, J. Balzarini, *J. Med. Chem.* **2002**, *45*, 1918–1929; b) A. Holý, J. Günter, H. Dvořáková, M. Masojídková, G. Andrei, R. Snoeck, J. Balzarini, E. De Clercq, *J. Med. Chem.* **1999**, *42*, 2064–2086.
[10] A. Holý, *Curr. Pharm. Des.* **2003**, *9*, 2567–2592.
[11] H. Sigel, *Chem. Soc. Rev.* **2004**, *33*, 191–200.
[12] A. Fernández-Botello, R. B. Gómez-Coca, A. Holý, V. Moreno, H. Sigel, *Inorg. Chim. Acta* **2002**, *331*, 109–116.
[13] O. Yamauchi, A. Odani, H. Masuda, H. Sigel, *Met. Ions Biol. Syst.* **1996**, *32*, 207–270.
[14] T. J. Matray, E. T. Kool, *J. Am. Chem. Soc.* **1998**, *120*, 6191–6192.
[15] *Handbook on Metalloproteins* (Eds.: I. Bertini, A. Sigel, H. Sigel), M. Dekker, Inc., New York, **2001**, pp. 709–880.
[16] A. E. Palmer, R. K. Szilagyi, J. R. Cherry, A. Jones, F. Xu, E. I. Solomon, *Inorg. Chem.* **2003**, *42*, 4006–4017.
[17] E. I. Solomon, U. M. Sundaram, T. E. Machonkin, *Chem. Rev.* **1996**, *96*, 2563–2605.
[18] E. I. Solomon, P. Chen, S. K. Lee, M. Metz, A. E. Palmer, *Angew. Chem. Int. Ed.* **2001**, *40*, 4570–4590.
[19] E. W. Ainscough, A. M. Brodie, J. D. Ranford, J. M. Waters, *J. Chem. Soc., Dalton Trans.* **1997**, 1251–1256.
[20] a) S. J. Langley, M. Helliwell, R. Sessoli, P. Rosa, W. Wernsdorfer, R. E. P. Winpenny, *Chem. Commun.* **2005**, 5029–5031; b) H. C. Yao, J. J. Wang, Y. S. Ma, O. Waldmann, W. X. Du, Y. Song, Y. Z. Li, L. M. Zheng, S. Decurtins, X. Q. Xin, *Chem. Commun.* **2006**, 1745–1747; c) M. Shanmugam, M. Shanmugam, G. Chastanet, R. Sessoli, T. Mallah, W. Wernsdorfer, R. E. P. Winpenny, *J. Mater. Chem.* **2006**, *16*, 2576–2578.
[21] J. Pons, X. López, J. Casabó, F. Teixidor, A. Caubet, J. Rius, C. Miravitlles, *Inorg. Chim. Acta* **1992**, *195*, 6–66.
[22] J. Pons, A. Chadghan, A. Alvarez-Larena, J. F. Piniella, J. Ros, *Inorg. Chem. Commun.* **2001**, *4*, 610–612.
[23] C. Janiak, *J. Chem. Soc., Dalton Trans.* **2000**, 3885–3896.
[24] a) R. W. Gellert, R. Bau, *Met. Ions Biol. Syst.* **1979**, *8*, 1–55; b) K. Aoki, *Met. Ions Biol. Syst.* **1996**, *32*, 91–134.
[25] a) R. P. Doyle, P. E. Kruger, B. Moubaraki, K. S. Murray, M. Nieuwenhuyzen, *Dalton Trans.* **2003**, 4230–4237; b) S. Youngme, P. Phuengphai, N. Chaichit, G. A. van Albada, O. Roubeau, J. Reedijk, *Inorg. Chim. Acta* **2005**, *358*, 849–853.
[26] A. Holý, M. Buděšinský, J. Podlaha, I. Cisařová, *Collect. Czech. Chem. Commun.* **1999**, *64*, 242–256.
[27] G. M. Sheldrick, *A Computer Program for the Determination of Crystal Structures*, **1997**, University of Göttingen, Germany.
[28] *International Tables of X-ray Crystallography*, **1974**, Ed. Kynoch Press, vol. IV, pp 99–100 and 149.

Received: October 24, 2006